

Fourier Transform Microwave Spectrum of Propene-3- d_1 ($\text{CH}_2=\text{CHCH}_2\text{D}$), Quadrupole Coupling Constants of Deuterium, and a Semiexperimental Equilibrium Structure of Propene

Jean Demaison,^{*,†} Norman C. Craig,^{*,†} Ranil Gurusinghe,[‡] Michael J. Tubergen,[‡] Heinz Dieter Rudolph,[†] Laurent H. Coudert,[¶] Péter G. Szalay,[§] and Attila G. Császár[#]

[†]Section of Chemical Information Systems, University of Ulm, Albert Einstein Allee 47, 89069 Ulm, Germany

[‡]Department of Chemistry and Biochemistry, Oberlin College, Oberlin, Ohio 44074, United States

[‡]Department of Chemistry, Kent State University, Kent, Ohio 44242, United States

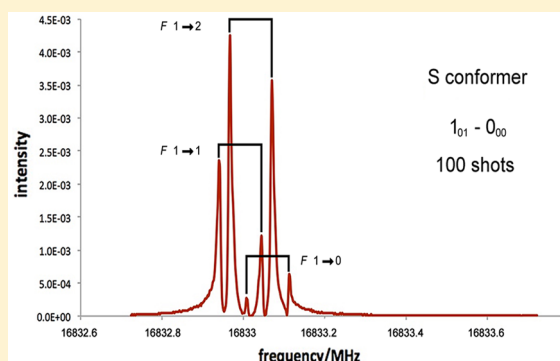
[¶]Institut des Sciences Moléculaires d'Orsay, UMR 8214, Bâtiment 210, Université Paris-Sud, 91405 Orsay, France

[§]Institute of Chemistry, Eötvös Loránd University, Budapest H-1053, Hungary

[#]MTA-ELTE Complex Chemical Systems Research Group, Pázmány Péter sétány 1/A, Budapest H-1117, Hungary

S Supporting Information

ABSTRACT: The ground-state rotational spectrum of propene-3- d_1 , $\text{CH}_2=\text{CHCH}_2\text{D}$, was measured by Fourier transform microwave spectroscopy. Transitions were assigned for the two conformers, one with the D atom in the symmetry plane (S) and the other with the D atom out of the plane (A). The energy difference between the two conformers was calculated to be 6.5 cm^{-1} , the S conformer having lower energy. The quadrupole hyperfine structure due to deuterium was resolved and analyzed for both conformers. The experimental quadrupole coupling and the centrifugal distortion constants compared favorably to their ab initio counterparts. Ground-state rotational constants for the S conformer are 40582.157(9), 9067.024(1), and 7766.0165(12) MHz. Ground-state rotational constants for the A conformer are 43403.75(3), 8658.961(2), and 7718.247(2) MHz. For the A conformer, a small tunneling splitting (19 MHz) due to internal rotation was observed and analyzed. Using the new rotational constants of this work as well as those previously determined for the ^{13}C species and for some deuterium-substituted species from the literature, a new semiexperimental equilibrium structure was determined and its high accuracy was confirmed. The difficulty in obtaining accurate coordinates for the out-of-plane hydrogen atom is discussed.



1. INTRODUCTION

Propene is the second simplest member of the alkene class of hydrocarbons, and its CH_3 group is an internal rotor. Propene is released by vegetation, and it is also a byproduct of combustion. It has important industrial applications, for instance, the synthesis of polypropylene. In 2007, it was found in the dark cloud TMC-1¹ and, quite recently, in the stratosphere of Titan by the Cassini orbiter spacecraft.²

Propene spectra have been extensively studied in different electromagnetic regions and at different resolutions. In particular, the microwave (MW) spectrum of propene was investigated as early as 1957.³ This initial report was followed by many studies, which are summarized in ref 4. In 2008, a semiexperimental (SE) equilibrium structure, r_e^{SE} , was determined by two of the present authors using the then available rotational constants of 20 isotopologues.⁵ In the same work, the structure was compared to results of high-level ab initio electronic structure computations. The accuracy of the SE

structure was limited by the lack of good A rotational constants for most isotopologues.

Propene is a near-prolate molecule with a large A rotational constant (about 46 GHz for the parent species) and a very small component of the dipole moment along the principal axis b, $\mu_b = 0.05(2)\text{ D}$.³ An accurate determination of the axial A rotational constant is difficult because it requires measurement of very weak b-type lines. Few observable b-type lines are in the 10–22 GHz range covered by our previous study and the current one, but a number are in the whole range. Recently, deficiencies in MW data prompted a new investigation of the MW spectra of the three ^{13}C isotopic species by means of a pulsed-jet supersonic expansion Fourier transform spectrometer of the Balle–Flygare design.⁴ In the present work, we report new measurements of the centimeter-wave spectrum of

Received: February 14, 2017

Revised: March 31, 2017

Published: April 3, 2017

the two conformers of propene-3- d_1 ($\text{CH}_2=\text{CHCH}_2\text{D}$) with the same technique.

With improved rotational constants available for the three ^{13}C isotopologues and for the conformers of $\text{CH}_2=\text{CHCH}_2\text{D}$, the stage is set for determining an improved SE equilibrium structure of propene. In doing so, we make use of the mixed regression method that has come to the fore in recent years.⁶ Determination of the structures of 2-deoxyribose and fructose is our most recent example,⁷ which includes references to other applications of this method. One goal of this new work is to try to understand why it is difficult to determine accurately the geometry of a methyl group using data for an asymmetrically deuterated species CH_2D .⁸ Recently, Piccardo et al. reported a comprehensive determination of SE structures for 47 organic molecules, including propene, with vibration–rotation constants computed with DFT methods.⁹

2. EXPERIMENTAL SECTION

2.1. Synthesis. Propene-3- d_1 was prepared by reaction of allylmagnesium chloride and deuterium oxide. Deuterium oxide (Aldrich, 99.9%) was dripped into 10 mL of well-stirred 2 M allylmagnesium chloride dissolved in tetrahydrofuran (THF, Aldrich) at room temperature. A slow flow of pure He gas (5.0 grade, O. E. Meyer, Sandusky, OH) carried the reaction products through a U-tube trap cooled to $-50\text{ }^\circ\text{C}$ to condense THF. Because propene boils at $-48\text{ }^\circ\text{C}$, a dry ice–acetone mixture was inappropriate to condense THF; too much propene would be condensed. The temperature of $-50\text{ }^\circ\text{C}$ is just below the $-48\text{ }^\circ\text{C}$ boiling point of propene. The flow of helium gas carried the products into a second, larger trap cooled with liquid nitrogen, where the propene condensed. Yields varied from 80 to 90%. Collected propene-3- d_1 was dried by distillation through a tube packed with phosphorus pentoxide dispersed on glass wool. An infrared spectrum of propene-3- d_1 in the gas phase is given in Figure S1a,b in the [Supporting Information](#). This spectrum shows a negligible amount of the THF solvent.

2.2. Gas Mixtures for Microwave Spectroscopy. Gas mixtures for MW spectroscopy were prepared by condensing samples of propene-3- d_1 up to 12 mmol in a 2 L flask. Pure He (Airgas) or He/Ne (30/70, Airgas) gas was supplied to a pressure of 203 kPa. When the gas pressure dropped to ~ 173 kPa, driver gas was added to restore the pressure to 203 kPa. Up to 10 such additions of driver gas were made in an experiment. Propene-3- d_1 was recovered from the mixtures with He or He/Ne used in MW spectroscopy by passing the gas very slowly through a glass helix (18 turns, 2.75 cm diameter) cooled with liquid nitrogen. Recovered propene-3- d_1 was dried by distillation through the P_2O_5 column before reuse.

2.3. Microwave Spectroscopy. The pulsed jet, mini-FT MW instrument at Kent State University was used for the observations. This instrument is of the Balle–Flygare design, as modified by Suenram et al.¹⁰ Details of the Kent instrument, which spans the frequency range of 10–22 GHz, have been reported.¹¹ The pulsed nozzle is mounted near the center of the fixed mirror to give a sample beam collinear with a MW pulse. Thus, Doppler doublets occur for observed lines. Doppler splitting is $\sim 50\%$ larger with pure helium than with the He/Ne mixture. Filtering of FIDs was minimized to improve observation of deuterium splitting. Uncertainty in the measurements was 2.4 kHz due to digital frequency resolution.

3. COMPUTATIONAL DETAILS

3.1. Electronic Structure Computations. Various electronic structure techniques were applied in this study. Kohn–Sham density functional theory (DFT)¹² using Becke’s three-parameter hybrid exchange functional¹³ and the Lee–Yang–Parr correlation functional,¹⁴ together denoted as B3LYP, was used extensively. It is now well-established that DFT provides reasonably accurate vibrational frequencies at low cost. Good results for structures are usually obtained with the B3LYP method.^{15,16} The correlation-consistent polarized valence triple- ζ basis set, cc-pVTZ,¹⁷ was chosen for the B3LYP computations.

Most of the electronic structure computations were made at the level of second-order Møller–Plesset perturbation theory (MP2)¹⁸ with the cc-pVTZ basis set in the frozen core approximation. The coupled cluster (CC) technique with single and double excitations¹⁹ and a perturbative treatment of connected triples, CCSD(T),²⁰ was also employed. The CCSD(T) computations utilized a mixed atom-centered Gaussian basis set, composed of cc-pVTZ on H and either cc-pVQZ¹⁷ (together designated as cc-pV(Q,T)Z) or the correlation-consistent polarized weighted core–valence quadruple- ζ , cc-pwCVQZ²¹ on C (together designated as cc-pwCV(Q,T)Z). For the CCSD(T) computations, all electrons were correlated.

Preliminary values of the quadrupole coupling constants were calculated at the B3LYP level of theory with the split-valence 6-311+G(3df,2pd) basis set, as implemented in Gaussian09 (G09).²²

All electronic structure computations were performed with the codes Gaussian 03 or G09²² and CFOUR.^{23–25}

3.2. Hamiltonian. A centrifugal-distorted Hamiltonian complete up to quartic terms in the asymmetric top reduction and the I representation was used to fit the new propene-3- d_1 spectra.²⁶ As propene is a near-prolate top, it might seem more appropriate to use the symmetric top reduction. However, for the parent species, both reductions give fits of the same quality. Therefore, to make a direct comparison with the constants of the other isotopologues, asymmetric top reduction was preferred.

In the asymmetric conformer of the $\text{CH}_2\text{CHCH}_2\text{D}$ species, most rotational lines are split into double clusters. Although it is possible to fit their mean frequency with the standard Watson Hamiltonian, another approach was used in order to account for the splitting and to check that the rotational constants are not perturbed by a large-amplitude torsional motion. For this goal, a phenomenological Internal Axis Method (IAM) Hamiltonian was chosen, which accounts for the rotational dependence of the splitting. This Hamiltonian is described in ref 27, and it is based on the water dimer formalism.^{28,29} In addition to the standard rotational constants and the centrifugal distortion constants, three parameters are needed: h_{12} is half of the tunneling splitting of the levels for $J = 0$, and the angles θ_{12} and φ_{12} describe the rotational dependence of the tunneling splitting. All of these parameters are introduced in eqs 12 and 13 of ref 27.

Deuterium has a spin $I = 1$ and therefore a nuclear quadrupole moment. The consequent hyperfine structure from quadrupole–rotation interaction was analyzed with first-order perturbation theory.³⁰ The diagonal quadrupole coupling constants, $\chi_+ = \chi_{bb} + \chi_{cc}$ and $\chi_- = \chi_{bb} - \chi_{cc}$, were fitted by a linear least-squares procedure to the observed splittings.

Deperturbed lines were used in fitting the rotational Hamiltonians.

4. RESULTS

4.1. Electronic Structure Results. The energy difference between the two conformers of $\text{CH}_2=\text{CHCH}_2\text{D}$ was

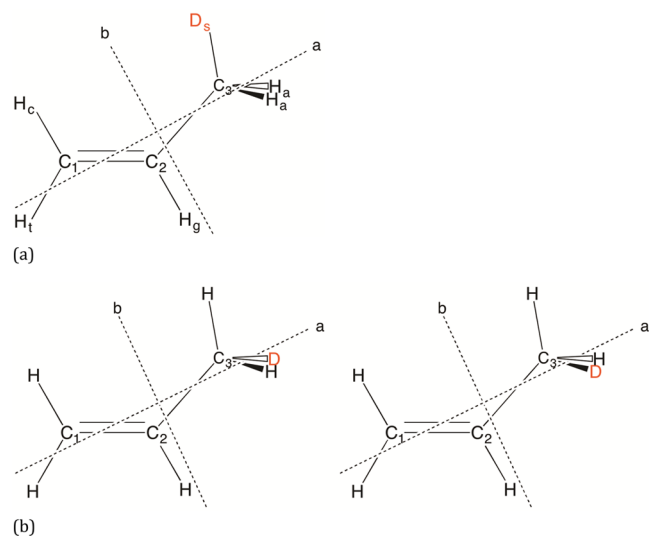


Figure 1. Schematic structures of the S (a) and A (b) conformers of propene-3- d_1 . Dotted lines show the approximate orientations of the *a* and *b* principal axes of rotation, which lie in the symmetry plane for the S conformer but are tipped somewhat out of this plane toward the D atom for the A conformers.

calculated as the difference between zero-point vibrational energies (ZPEs) by employing MP2/cc-pVTZ anharmonic force fields. The CH_2D_s conformer (*s* for CD in the plane of symmetry) is found to be lower in energy by 18 cal/mol (6.5 cm^{-1}). It has to be noted that this difference is quite small. Furthermore, the anharmonic contribution to the difference was found to be extremely small.

The potential energy function for internal rotation is expanded in a Fourier series compatible with the lower C_s symmetry

$$V(\alpha) = V_1 \frac{(1 - \cos \alpha)}{2} + V_2 \frac{(1 - \cos 2\alpha)}{2} + V_3 \frac{(1 - \cos 3\alpha)}{2} + \dots$$

where α is the angle of internal rotation of the CH_2D methyl top with respect to the $\text{CH}_2=\text{CH}$ frame; α is taken equal to zero for the CH_2D_s conformer.

The energy difference, 6.5 cm^{-1} , which is then $0.75(V_1 + V_2)$, shows that the dominant term in the potential energy is $V_3 = 1975 \text{ cal/mol}$, whose value was computed at the all-electron CCSDT(T)/cc-pwCV(Q,T)Z level. The small ZPE correction to the difference in energy was obtained using the harmonic force field calculated at the same level of theory. The result for V_3 is in fair agreement with the available experimental values (in cal/mol): 1963³¹ or 1956.³² The structure of the transition state corresponding to the maximum of the barrier is given in Table S1. The main difference compared to the low-energy form is an elongation of the C–C single bond, presumably due to repulsion of the in-plane hydrogen atoms.

The experimental ground-state centrifugal distortion constants are compared with the computed equilibrium ones in Table S2. This comparison gives a check of the quality of the

quadratic and cubic parts of the force field. For the quartic constants, the different force fields give almost identical results, and the agreement is good with the experimental values, except, as usual, for δ_K . The value of δ_K is quite sensitive to the ab initio values of the rotational constants used in the calculation, values that are significantly different at each level of theory.

As to the sextic centrifugal distortion constants, the agreement is also good between the different force fields with the exception of the nondiagonal constants φ_{JK} and φ_K , which, like δ_K , are difficult to calculate accurately. A comparison with the experimental values is compromised because the constant φ_{JK} could not be determined accurately. Nevertheless, the agreement between experiment and theory is good for the constants Φ_J , Φ_{KJ} , Φ_K and φ_J . The only significant discrepancy is with Φ_{JK} , whose experimental value is about twice the calculated values. However, it is interesting to note that fixing Φ_{JK} at the CCSD(T)/cc-pV(Q,T)Z value, -0.27 Hz , in the fit gives $\varphi_K = -7.06(19) \text{ Hz}$, in excellent agreement with the CCSD(T) value. Table S2 includes the centrifugal distortion constants for this alternative fit to the observations. In conclusion, the apparent discrepancy may be explained by a high correlation between Φ_{JK} and φ_K .

The harmonic, ω_i , and the anharmonic, ν_i , vibrational wavenumbers for $\text{CH}_2=\text{CHCH}_3$ are given in Table S3. The experimental wavenumbers come from Es-sebbar et al.³³ The agreement between the calculated and the experimental vibrational frequencies ν_i is rather good, the median of absolute deviations (MAD) being only 1.8 cm^{-1} with the CCSD(T)/cc-pV(Q,T)Z force field. Obviously, it is larger for the MP2 and B3LYP force fields that are of similar quality. The MAD for the MP2/aug-cc-pVTZ results (7.2 cm^{-1}) is somewhat smaller than the MAD for the MP2/cc-pVTZ model (7.7 cm^{-1}). We note that the overall differences between the anharmonic frequencies and the harmonic frequencies (i.e., corrections) calculated at either the MP2/cc-pVTZ level or the CCSD(T)/cc-pV(Q,T) level are quite small; the MAD difference is only 2.3 cm^{-1} , with, however, two large differences for the CH stretch and the CH_2 sym stretch, 30 and 44 cm^{-1} , respectively. In conclusion, the MP2/cc-pVTZ level of theory may be considered accurate enough to compute the cubic force field needed for calculation of the vibration–rotation constants (α).

Experimental α constants have been determined for the B and C rotational constants of the torsional mode (ν_{21}) of three isotopologues. They are compared with their ab initio counterparts in Table S4. This comparison is particularly interesting because the torsion may be considered as a well-isolated mode that is not perturbed by anharmonic resonances. However, it is probably a large-amplitude motion, which could severely affect the accuracy of the anharmonic force field. The comparison is made for the parent species for which three different force fields are available (two for the $\text{CHD}_t=\text{CHCH}_3$ isotopologue and one for the $\text{CH}_2\text{C}=\text{CDCH}_3$ isotopologue). The agreement is comparable or better than that found for other molecules without large-amplitude motion, such as vinyl halides.^{34–36} Furthermore, the different force fields appear to be of similar quality. Thus, we conclude that, in the case of propene, the torsion behaves as a small-amplitude, nearly harmonic vibration, which is not unexpected due to the smallness of the tunneling splitting.

A last useful comparison is for the sums of the rovibrational corrections needed to adjust the ground-state rotational constants to obtain the SE equilibrium rotational constants. These corrections are given in Table S5 for the parent and a

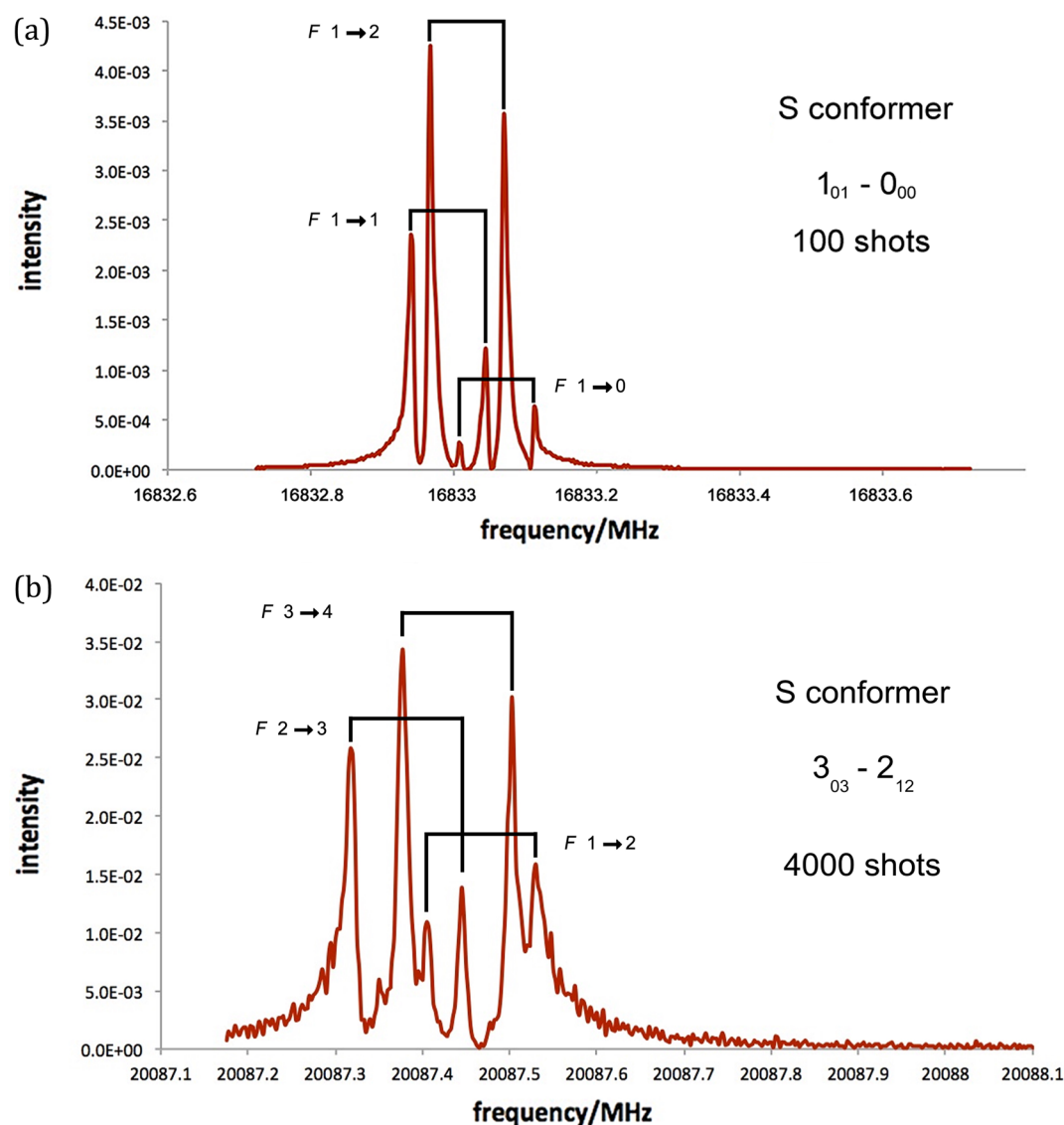


Figure 2. MW observations for the S conformer of propene-3-*d*₁. (a) 1₀₁–0₀₀ transition with He driver gas. (b) 3₀₃–2₁₂ transition with He/Ne driver gas. Links designate Doppler doublets.

Table 1. Deperturbed Rotational Frequencies^a of the S Conformer of Propene-3-*d*₁ (in MHz)

<i>J</i> '	<i>K</i> ' _a	<i>K</i> ' _c	<i>J</i> ''	<i>K</i> '' _a	<i>K</i> '' _c	$\nu_{\text{depert.}}$	obs – calc	σ^b
1	0	1	0	0	0	16833.015	0.000	5
2	1	2	1	1	1	32364.930 ^c	–0.052	100
2	0	2	1	0	1	33626.410 ^c	–0.009	100
2	1	1	1	1	0	34966.940 ^c	–0.047	100
3	0	3	2	1	2	20087.426	0.000	5
4	1	3	4	1	4	13004.141	0.000	5
5	2	3	6	1	6	10970.412	–0.016	30
5	1	4	5	1	5	19492.339	0.001	5
6	1	5	5	2	4	17651.580	–0.019	30
9	2	7	9	2	8	12001.043	0.000	5
10	2	8	10	2	9	17397.364	0.000	5

^aFor the experimental frequencies of the hyperfine components, see Table 2. ^bUncertainty in kHz used for the weighting. ^cThe three *J* = 1 → 2 transitions with unresolved splittings are from ref 38.

critical deuterium species. The comparison between the parent species and the CHD₁=CHCH₃ deuterated species is

noteworthy because the deuterium atom is the farthest one from the center of mass. It is found that the difference between the MP2/cc-pVTZ and CCSD(T)/cc-pV(Q,T)Z force field results for each principal axis is small and almost constant. This agreement indicates that the two force fields should give nearly the same SE structure.⁸

The general conclusion of these comparisons is that the MP2/cc-pVTZ cubic force field should permit calculating adequate SE equilibrium rotational constants.

4.2. Microwave Spectra. Propene-3-*d*₁ consists of two conformers. Figure 1 gives schematic structures for the two conformers. In the S conformer, Figure 1a, the CD bond eclipses the C=C bond. This conformer gives single clusters of rotational transitions well described by the rigid rotor approximation.²⁷ The A conformer, Figure 1b, has the CD bond out of the symmetry plane of the S conformer. Because two forms of the A conformer exist, its spectrum consists of two clusters for each transition, which are a consequence of tunneling. These doublets are designated as (+) and (–).

4.2.1. Microwave Spectrum of the S Conformer of Propene-3-*d*₁. Figure 2 gives examples of traces for MW

Table 2. Nuclear Quadrupole Hyperfine Structure for the S Conformer of Propene-3- d_1 (All Frequencies in MHz)

$J'K_a'K_c' - J''K_a''K_c''$	F'	F''	ν_{obs}	ν_{HFS}	
				obs ^a	obs - calc
101-000	0	1	16833.062	0.042	-0.001
	1	1	16832.991	-0.029	0.000
	2	1	16833.020		
303-212	2	1	20087.468	0.028	0.001
	3	2	20087.381	-0.059	-0.001
	4	3	20087.440		
413-414 ^b	3	3	13004.195	0.030	0.005
	4	4	13004.069	-0.096	0.002
	5	5	13004.165		
514-515 ^c	4	4	19492.390	0.024	0.004
	5	5	19492.266	-0.100	0.000
	6	6	19492.366		
927-928	9	9	12001.020	-0.038	0.004
	8	8	12001.058		
	10	10	12001.058		
1028-1029	11	11	17397.389	0.050	0.002
	10	10	17397.339		
	9	9	17397.339		

^aWith respect to the strongest component of the hyperfine splitting.

^bAdditional lines presumably due to spin-spin splitting: 13004.053 and 13004.179 MHz. ^cAdditional lines presumably due to spin-spin splitting: 19492.246 and 19492.375 MHz.

Table 3. Ground-State Rotational Parameters for the S Conformer of Propene-3- d_1

parameter	unit	experimental ^a	ab initio ^b
A	MHz	40 582.1573(89)	
B	MHz	9067.0238(11)	
C	MHz	7766.0165(12)	
Δ_J	kHz	6.359(24)	6.499
Δ_{JK}	kHz	-26.97(13)	-28.46
Δ_K	kHz	311.2(1.2)	306.1
δ_J	kHz	1.3454(22)	1.3811
δ_K	kHz	-9.52(16)	-5.35
χ_{aa}	MHz	-0.095(4)	-0.0961
χ_{bb}	MHz	0.192(4)	0.1981
χ_{cc}	MHz	-0.097(3)	-0.102
χ_{ab}	MHz	-	-0.0099

^aAb initio values of Δ_J , Δ_{JK} , and Δ_K used as predicates; see the text.

^bMP2/cc-pVTZ values for the distortion constants and B3LYP/6-311+G(3df,2pd) values for the quadrupole coupling constants.

transitions for the S conformer of propene-3- d_1 . Figure 2a is the strong $1_{01}-0_{00}$ a -type transition, recorded in 100 shots; Figure 2b is the weak $3_{03}-2_{12}$ b -type transition, recorded in 4000 shots. Intensities are in arbitrary units. Deuterium quadrupolar coupling splits both transitions, as designated with F quantum numbers. Helium driver gas caused a larger Doppler splitting ($\sim 50\%$ greater compared to He/Ne) for the $1_{01}-0_{00}$ transition. Table 1 gives the deperturbed transitions derived from the observations. All but three of the transitions are a -type. The b -type transitions are important in defining the A_0 rotational constant.

The observed nuclear quadrupole splittings listed in Table 2 were fitted to determine the quadrupole coupling constants; their values are given in Table 3 in comparison with the ab initio values. Using the molecular structure determined in

section 5, we can calculate the value of the quadrupole coupling constant along the C-D bond. This value is 193 kHz, close to the value found for CH_3D , 191.5(8) kHz.³⁷ Finally, the deperturbed frequencies were calculated (Table 1). The three a -type transitions observed unsplit by Lide and Christensen by Stark spectroscopy are included in Table 1.³⁸ To strengthen the data set, these three $J = 1 \rightarrow 2$ transitions with reduced weight were included in fitting the rotational constants.

An initial fit to the 11 MW lines with all five quartic centrifugal distortion constants as well as the three rotational constants free permitted a determination of all 8 parameters. However, this fit appeared as ill-conditioned, with Δ_J , Δ_K , and δ_K being almost fully correlated with A and B . To circumvent this difficulty, the method of predicate observations (POs) was used. In the PO method, the experimental frequencies are fitted together with appropriately weighted ab initio (predicate) values for the centrifugal distortion constants. A very satisfactory fit was obtained using three predicates for Δ_J , Δ_{JK} , and Δ_K , the uncertainty used to determine their weight being 10% of their value. The last column in Table 1 gives the obs - calc values obtained in the fitting. Table 3 gives the rotational constants fit to the transitions.

The new rotational constants for the S conformer are close to the values predicted from Tables 5 and 6 in Demaison and Rudolph's previous determination of the structure of propene.⁵ When the error in the fit of the equilibrium rotational constants in Table 6 of ref 5 is applied to the observed ground-state rotational constants in Table 5 of ref 5, the predicted values are $A_0 = 40588$, $B_0 = 9066.7$, and $C_0 = 7766.0$ MHz, which compare favorably with the new values of 40582.16, 9067.02, and 7766.02 MHz, respectively.

4.2.2. Microwave Spectrum of the A Conformer of Propene-3- d_1 . Figure 3 shows two of the traces for MW transitions of the A conformer of propene-3- d_1 . Figure 3a is the strong $1_{01}-0_{00}$ transition, recorded in 100 shots; Figure 3b is the weaker $5_{14}-5_{15}$ transition, recorded in 2000 shots. The two components of the $5_{15}-5_{14}$ transition are indicated in the figure. The stronger cluster on the left with lines connecting the Doppler doublets is the (-) component. The weaker cluster on the right is the (+) component. This component was seen with greater intensity in a separate scan by moving the MW pump frequency closer to the transition. The splitting pattern was the same as that for the (-) component. Table 4 contains all of the transitions observed in the present work in the 10-22 GHz region. The (+) and (-) designations come from Hirota and co-workers³⁹ or by analogy with Pearson et al.'s assignments for propene.⁴¹ The new observations have higher precision and accuracy than their prior observation by Hirota et al.³⁹ Table 5 contains deperturbed values of new observations as well as older observations. Lines for $J = 1 \rightarrow 2$ are averages of observations by Lide and Christensen³⁸ and Hirota et al.³⁹ Some other lines observed by Hirota et al. are included in Table 5.^{39,40} The older observations were given reduced weight in fitting the rotational constants.

The nuclear quadrupole splittings listed in Table 4 were fitted separately for each component of the two clusters to determine the quadrupole coupling constants whose values are given in Table 6 along with their ab initio counterparts.

The mean frequency of each doublet was calculated and fit to a Watson Hamiltonian. Table 6 reports the rotational and centrifugal distortion constants for the A conformer. All of the constants are well determined.

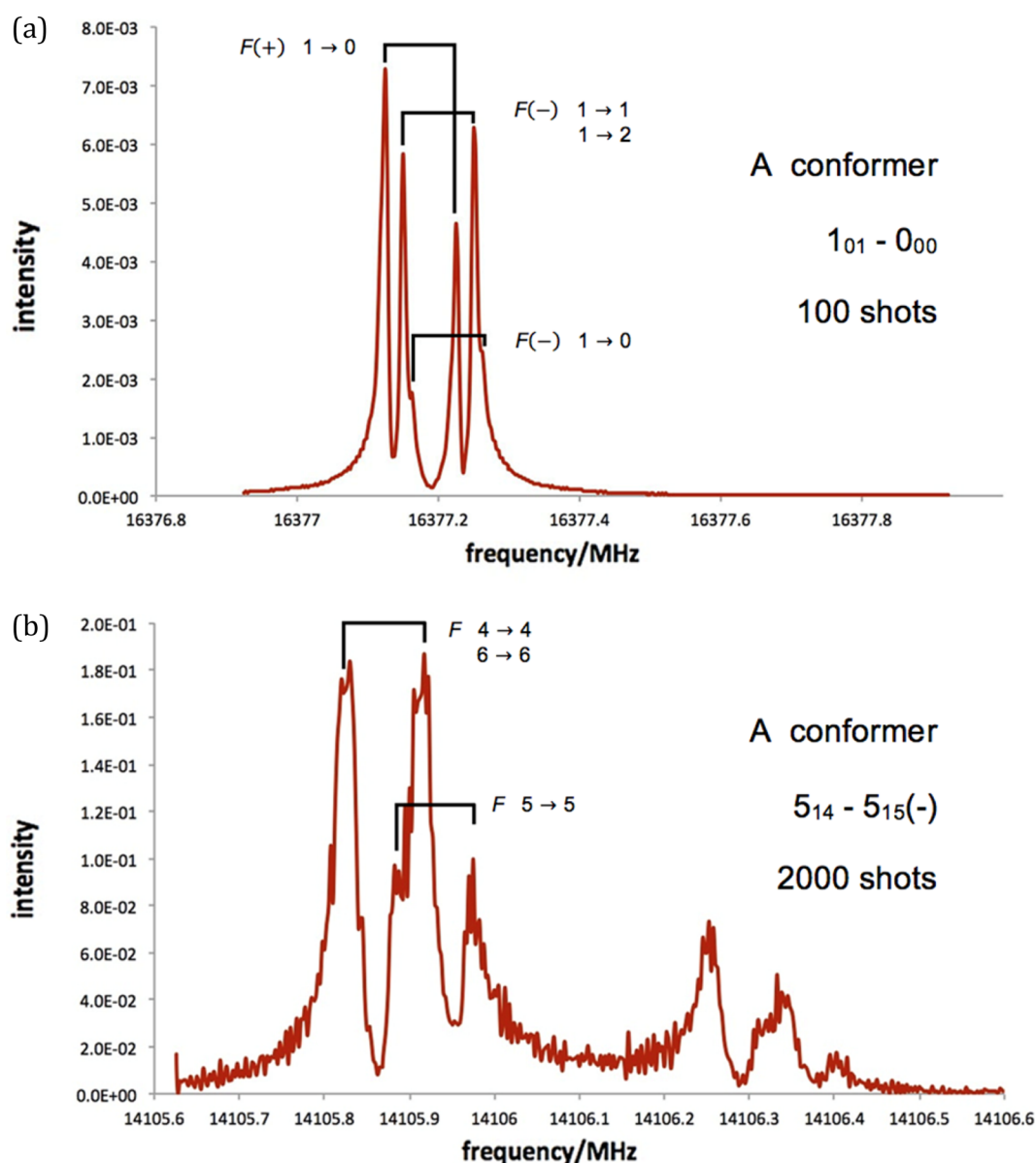


Figure 3. MW observations for the A conformer of propene-3-*d*₁ with He/Ne driver gas. (a) $1_{01} - 0_{00}$ transition, in which the two components overlap. Poorly resolved shoulders on the low-frequency sides of the lowest pair are not designated. (b) $5_{14} - 5_{15}$ transition consisting of two components with the stronger (–) component on the left showing linked Doppler doublets. The weaker (+) component to the right was observed better with the MW pump frequency moved closer.

The transitions were also fit using the IAM Hamiltonian introduced in ref 27, and the tunneling parameters h_{12} , θ_{12} , and φ_{12} were determined in addition to the rotational and centrifugal distortion constants. The results are also given in Table 6. It is worth noting that the two fitting approaches give almost identical rotational constants as well as compatible quartic centrifugal distortion constants, which are furthermore in good agreement with the ab initio predictions. It is possible to compute the tunneling parameters θ_{12} and φ_{12} , as in section 3 of ref 27, using eq 49 of Hougen²⁸ and making a reasonable assumption about the geometry of the molecule along the tunneling path connecting the two A conformers. The calculated values are also reported in Table 6. Experimental and calculated values of θ_{12} and φ_{12} are within 0.2 and 0.02°, respectively. Taking into account that the calculated values are equilibrium values whereas experimental values are ground-state values, the agreement is satisfactory, especially for φ_{12} . It

further confirms that the large-amplitude motion displayed by propene-3-*d*₁ is indeed a 120° rotation of the monodeuterated methyl group.

As for the S conformer, the new rotational constants can be compared with those predicted in the work of Demaison and Rudolph.⁵ The predictions from this previous work give $A_0 = 43378$, $B_0 = 8659.3$, and $C_0 = 7718.4$ MHz. The new values for the rotational constants are 43403.75, 8658.96, and 7718.25 MHz, in good agreement with the predictions.

4.3. Semiexperimental Equilibrium Structure. The r_e^{SE} of propene was determined several years ago using the rotational constants of 20 isotopologues.⁵ Although the parameters obtained are reliable, they suffer from several weaknesses. In particular, the deviations of the A(SE) rotational constants from the ones calculated from experimental values are substantial. These discrepancies are due to experimental ground-state rotational constants of the isotopologues being

Table 4. Nuclear Quadrupole Hyperfine Structure for the A Conformers of Propene-3- d_1 (All Frequencies in MHz)

$J'K'_a'K'_c'-J''K''_a''K''_c''$	F'	F''	ν_{HFS}			ν_{HFS}		
			ν_{obs}	obs ^a	obs – calc	ν_{obs}	obs ^a	obs – calc
101–000	0	1	16377.175	A(+) Component		16377.212	A(–) Component	
	1	1	16377.168	0.007	0.000	16377.200	0.012	0.000
	2	1						
303–212 ^b	3	2	15231.790	0.022	0.001	15235.031	0.022	0.000
	4	3	15231.768			15235.009		
514–515	5	5	14106.359	0.064	0.002	14105.930	0.061	–0.002
	4	4	14106.295			14105.869		
	6	6	14106.295					
615–616	6	6	19737.452	0.060	–0.002	19736.855	0.065	0.002
	5	5	19757.392			19736.790		
	7	7	19757.392					
1129–11210	11	11	12481.219	0.022	–0.001	12481.542	0.023	–0.001
	10	10	12481.197			12481.519		
	12	12	12481.197					
12210–12211	12	12	17018.532	0.027	0.001	17018.926	0.026	–0.001
	10	10	17018.505			17018.900		
	9	9	17018.505					

^aWith respect to the strongest component of the hyperfine splitting. ^bAdditional lines at 15231.758 MHz for A(+) and 15234.998 MHz for A(–).

determined from very few lines and A_0 not being properly determinable. The recent measurement of MW lines for the three ^{13}C isotopologues as well as the results for the two CH_2D species of the present work should significantly improve the situation. Furthermore, there are two problems worth investigating. It can be difficult to determine accurately the position of some hydrogen atoms, in particular, the atoms far from the center of mass and a H atom of a methyl group.⁸

In the fits, two sets of ground-state rotational constants were used together. The first set, I, in Table S6 includes the parent species and the three ^{13}C species of ref 4 as well as the two CH_2D species of the present work. All of the constants of this set are believed to be accurate. The second set, II, in Table S6 whose constants are much less accurate, comprises the rotational constants of the further isotopologues determined in previous works and listed in ref 5. For this set II, only useful values of the B and C constants are available, and their accuracy is slightly worse than that for set I. Then, in order to estimate the weights used in the fits, each set was divided into three subsets, one for A, B, and C. The iteratively reweighted least-squares method⁶ was used in the fits; see Appendix I in the Supporting Information.⁶ The parameters obtained from the fit are precise; see Table 7, where they are compared to our previous r_e^{SE} and the Born–Oppenheimer (BO) equilibrium structure. Also given in Table 7 is the r_e^{SE} structure calculated with a B3LYP/SNSD force field by Piccardo et al.⁹ Although the SNSD basis set is only a double- ζ basis set developed for large molecular systems, the agreement with our r_e^{SE} structure is pleasing and confirms the accuracy of the vibration–rotation constants derived with the B3LYP/SNSD model. Compared to the results of ref 5, the increase of precision is more than a factor of 2. In particular, the internal coordinates of H_b , which is the atom farthest from the center of mass, are precise and in excellent agreement with the BO structure; see Table 7. This outcome is in agreement with the discussion of section 4.1, which concludes that the rovibrational corrections for $\text{CHD}_t=\text{CHCH}_3$ are accurate. It is also pleasing to note that the out-of-plane coordinate of H_a is extremely precise, $c(\text{H}_a) = 0.877874(4) \text{ \AA}$, and, furthermore, in excellent agreement with

the BO value. However, there are still two notable problems: (i) the residual for $A(\text{CH}_2\text{D}_a)$ is large, almost 12 MHz compared to a standard deviation of about 0.18 MHz for the other A constants of set I and (ii) one Cartesian coordinate derived from the rotational constants is not precise, $a(\text{H}_g) = -0.1414(19) \text{ \AA}$, the BO value being 0.139 \AA .

There are several possible explanations for the large residual of $A(\text{CH}_2\text{D}_a)$. First, the internal rotation was not taken into account when determining the rotational constants. One problem is that the semirigid rotor fit (internal rotation neglected) and the IAM fit, where the internal rotation is explicitly taken into account, give exactly the same value, as shown in section 4.2.2. Second, the two species CH_2D_s and CH_2D_a are quite close in energy. An interaction between these two species is possible. In this case, $A(\text{CH}_2\text{D}_s)$ should also be an outlier (with opposite sign), which it is not. Furthermore, analysis of the spectra does not indicate the existence of an interaction. Third, the method used to calculate the rovibrational corrections is inaccurate for a large-amplitude motion. Nevertheless, the values of the alphas are correctly calculated for $\text{CH}_2=\text{CHCH}_3$, $\text{CHD}_t=\text{CHCH}_3$, $\text{CH}_2=\text{CDCH}_3$, and $\text{CH}_2=\text{CHCH}_2\text{D}_s$. Thus, this explanation is unconvincing. However, comparing the residual to the rovibrational correction, 344 MHz, it appears that it is less than 3.5%. Although it is large, residuals of similar magnitude may be found for other molecules without large-amplitude motion. Indeed, statistical analysis of published results shows that, in the best cases, the error in $\alpha/2$ sums is about 2%, though it can be as large as 10%.⁴² In conclusion, the likeliest explanation for the outlying behavior of $A(\text{CH}_2\text{D}_s)$ is the lack of accuracy of the calculation of the rovibrational correction.

There are two additional ways to check the accuracy of the structure: with the help of the mixed regression method^{6,43} or by using Kraitchman's equations.⁴⁴ The method of mixed regression, also called the PO method, uses simultaneously equilibrium moments of inertia and bond lengths and bond angles from high-level quantum chemical calculations in the structure fitting.^{6,43} Generally, the PO method is used for large molecules, and the predicates are estimated without using the

Table 5. Rotational Frequencies^a of the A Conformer of Propene-3-*d*₁ (in MHz)

<i>J'</i>	<i>K'_a</i>	<i>K'_c</i>	<i>v'</i>	<i>J''</i>	<i>K''_a</i>	<i>K''_c</i>	<i>v''^a</i>	obs.	obs – calc ^b	σ^c
1	0	1	1	0	0	0	1	16377.174	0.000	10
1	0	1	0	0	0	0	0	16377.205	0.003	200
2	0	2	0	1	0	1	0	32735.358 ^d	–0.033	200
2	0	2	1	1	0	1	1	32735.358 ^d	–0.033	200
2	1	2	0	1	1	1	0	31813.382 ^d	–0.020	200
2	1	2	1	1	1	1	1	31813.382 ^d	–0.020	200
2	1	1	0	1	1	0	0	33695.184 ^d	–0.022	200
2	1	1	1	1	1	0	1	33695.184 ^d	–0.022	200
3	0	3	0	2	1	2	0	15231.773	–0.002	10
3	0	3	1	2	1	2	1	15235.012	0.001	10
3	0	3	0	2	0	2	0	49055.600 ^e	–0.081	200
3	0	3	1	2	0	2	1	49055.600 ^e	–0.081	200
3	2	1	0	2	2	0	0	49202.950 ^e	–0.024	200
3	2	1	1	2	2	0	1	49204.770 ^e	0.017	200
3	2	2	0	2	2	1	0	49133.400 ^e	–0.017	200
3	2	2	1	2	2	1	1	49135.280 ^e	0.103	200
4	1	3	0	4	1	4	0	9407.140 ^e	–0.031	200
4	1	3	1	4	1	4	1	9407.140 ^e	–0.031	200
4	2	3	0	5	1	4	0	16825.149	–0.002	10
4	2	3	1	5	1	4	1	16816.641	0.002	10
5	1	4	0	5	1	5	0	14106.316	0.001	10
5	1	4	1	5	1	5	1	14105.892	–0.003	10
6	1	5	0	6	1	6	0	19737.412	0.007	10
6	1	5	1	6	1	6	1	19736.812	–0.006	10
7	1	6	0	7	1	7	0	26292.145 ^e	0.025	100
7	1	6	1	7	1	7	1	26291.395 ^e	0.058	100
8	1	7	0	8	1	8	0	33757.075 ^e	–0.034	100
8	1	7	1	8	1	8	1	33756.045 ^e	–0.058	100
10	2	8	0	10	2	9	0	8831.430 ^e	–0.057	200
10	2	8	1	10	2	9	1	8831.430 ^e	–0.057	200
11	2	9	0	11	2	10	0	12481.204	–0.002	10
11	2	9	1	11	2	10	1	12481.525	0.001	10
12	2	10	0	12	2	11	0	17018.514	–0.005	10
12	2	10	1	12	2	11	1	17018.905	0.005	10
13	2	11	0	13	2	12	0	22500.295 ^e	0.043	200
13	2	11	1	13	2	12	1	22500.705 ^e	0.021	200
14	2	12	0	14	2	13	0	28961.310 ^e	–0.033	200
14	2	12	1	14	2	13	1	28961.790 ^e	–0.016	200
17	3	14	0	17	3	15	0	8370.245 ^e	–0.042	200
17	3	14	1	17	3	15	1	8370.755 ^e	–0.042	200
18	3	15	0	18	3	16	0	11444.315 ^e	–0.004	200
18	3	15	1	18	3	16	1	11445.025 ^e	0.063	200

^a*v''* = 0 for the A(+) component and 1 for the A(–) component. ^bCalculated from fit 2; see Table 6. ^cUncertainty in kHz used for the weighting. ^dAverage of refs 38 and 40. ^eReferences 39 and 40.

expensive CCSD(T) method. However, in the present case, we already have a very accurate BO structure that supplies predicates. To weight these predicates, an uncertainty of 0.001 Å was used for the C–H bond lengths, a conservative value of 0.002 Å was used for the CC bond lengths, and a value of 0.2° was used for the bond angles. The mixed estimation structure is given in the last column of Table 7. The structure is in excellent agreement with the structure without predicates, but as expected, the standard deviations of the parameters are slightly smaller. However, it is much more informative to look at the residuals of the two fits given in Table S6. The two sets of residuals are almost identical, the MAD of their differences being only 0.009 MHz. The only significant difference is for A(CH₂D₃), which has a residual of more than 11 MHz, but this datum is down-weighted and does not have any effect on the fit.

What is reassuring is that this large residual is almost the same in the two fits, 11.6 or 11.3 MHz. Furthermore, there is no systematic deviation in the residuals. This outcome is a corroboration of the good quality of the fit.

It is also instructive to look at the Cartesian coordinates derived from Kraitchman's equations.⁴⁴ These equations are not appropriate for determining an accurate SE structure because they are quite sensitive to the random errors of the rotational constants.^{45,46} Nevertheless, they allow one to make an estimate of an upper limit of the uncertainty of the Cartesian coordinates, and as they individually involve the rotational constants of only one isotopologue (besides those of the parent species), they permit checking the accuracy of the rotational constants. The details of the calculations are given in Appendix II in the Supporting Information, and the set of coordinates

Table 6. Ground-State Rotational Parameters for the A Conformer of Propene-3- d_1

parameter	unit	fit 1 ^a	fit 2 ^b	ab initio ^c
A	MHz	43 403.734(18)	43 403.751(27)	
B	MHz	8658.9617(22)	8658.9610(21)	
C	MHz	7718.2500(23)	7718.2468(19)	
Δ_J	kHz	5.312(50)	5.03(36)	5.413
Δ_{JK}	kHz	-15.960(80)	-12.32(83)	-17.578
Δ_K	kHz	424.6(2.2)	389.7(72)	400.3
δ_J	kHz	0.8426(22)	0.8496(22)	0.8761
δ_K	kHz	-59.34(23)	-58.94(20)	-46.44
Internal Rotation Parameters				
θ_{12}	deg		3.11412(18)	2.883 ^d
φ_{12}	deg		72.65011(87)	72.676 ^d
h_{12}	MHz		-9.532(45)	
Nuclear Quadrupole Coupling Constants				
$\chi_{aa}(A^+)$		-0.013(3)		-0.009
$\chi_{bb}(A^+)$		-0.076(3)		-0.072
$\chi_{cc}(A^+)$		0.089(3)		0.081
$\chi_{aa}(A^-)$		-0.021(3)		
$\chi_{bb}(A^-)$		-0.074(3)		
$\chi_{cc}(A^-)$		0.095(3)		

^aFit of the mean frequencies. ^bInternal axis method fit; see the text.

^cMP2/cc-pVTZ values for the distortion constants and B3LYP/6-311+G(3df,2pd) values for the quadrupole coupling constants.

^dValues obtained from the r_e^{BO} structure of the molecule along the tunneling path connecting the two A conformers.^{28,29}

derived for each atom substituted are in Table S7. The comparison of the coordinates is only meaningful for those calculated with the rotational constants of set I because the A constant is not well-known for the isotopologues of set II.

There are two discrepancies worth discussing. First, for atom C2, the a coordinate is $-0.1048(2)$ from the best fit, whereas Kraitchman's equation gives -0.1096 Å. The difference is large, 0.0048 Å. However, this coordinate is quite small, and a very small change of ΔP_a has a large influence on the coordinate. As shown in Appendix II, the uncertainty of the Kraitchman's coordinate is about 0.0034 Å. It is well documented that Kraitchman's equations are inaccurate for small coordinates.⁴⁶

Table 7. Structure of propene^a

method ^b	r_e^b	r_e (se) ^c			
		ref 5	ref 9	no predicate	14 predicates
basis					
C=C	1.3317	1.3310(7)	1.3326(2)	1.33156(35)	1.33148(26)
C-C	1.4954	1.4956(7)	1.4956(2)	1.49523(34)	1.49530(25)
CH _c	1.0825	1.0834(6)	1.0818(2)	1.08234(38)	1.08246(31)
CH _t	1.0804	1.0805(12)	1.0804(2)	1.08135(31)	1.08124(26)
CH _g	1.0845	1.0857(4)	1.0841(2)	1.08492(23)	1.08497(19)
CH _s	1.0888	1.0862(8)	1.0880(4)	1.08863(10)	1.088664(88)
CH _a	1.0907	1.0949(9)	1.0895(7)	1.09208(20)	1.09197(16)
CCC	124.481	124.47(2)	124.43(1)	124.4560(60)	124.4570(50)
CCH _c	121.149	121.08(5)	121.13(2)	121.156(22)	121.154(18)
CCH _t	121.455	121.55(14)	121.31(3)	121.398(39)	121.407(32)
CCH _g	118.856	118.75(13)	118.84(4)	118.75(12)	118.798(85)
CCH _s	111.027	111.10(4)	111.07(2)	111.027(14)	111.025(12)
CCH _a	110.972	110.53(11)	111.02(7)	110.877(26)	110.890(21)
CCCH _a	120.581	121.08(14)	120.47(8)	120.646(33)	120.627(27)

^aBond lengths are in Å, and bond angles are in degrees. Subscripts: g = geminal, c = cis to methyl, t = trans to methyl, s = in-plane H, and a = out-of-plane H. ^bCCSD(T)/VQZ + MP2[wCVQZ(ae) - wCVQZ] + MP2[V(Q₅Z) - VQZ] for CC bond lengths and the \angle (CCC) bond angle; for the other parameters: CCSD(T)/VQZ + MP2[wCVQZ(ae) - wCVQZ]. ^cSE structure.

Also interesting is the comparison of the coordinates for the out-of-plane hydrogen H_a. The fit gives (in Å) $a = -1.82375(8)$, $b = -0.1296(5)$, and $c = 0.87788(3)$, whereas Kraitchman's equations give $a = -1.8246(2)$, $b = -0.1259(3)$, and $c = 0.8765(5)$. Although the differences are small, the values are not fully compatible. This discrepancy is mainly due to the value of $A(\text{CH}_2\text{D})$, which is not compatible with the rotational constants of the other isotopologues. Using the P_c planar second moment of the parent species (or the ¹³C species or the CH₂D_s species) $I_c - I_a - I_b$ gives $c(\text{H}_a) = 0.8779$ Å, in perfect agreement with the value from the fit. Furthermore, there is also nice agreement between the structure from the fit and the BO structure. Finally, the accuracy of the CH_a bond length is confirmed by correlation with the isolated stretching frequency.⁵ Although the SE value of the $A(\text{CH}_2\text{D})$ rotational constant is obviously inaccurate, the use of the substitution Cartesian coordinates of Table S7 gives $r_c(\text{CH}_a) = 1.0901(11)$ Å and $\angle(\text{C2C3H}_a) = 111.09(14)^\circ$. These values, although less precise, are compatible with the results of the fit that gives for these two parameters $1.0920(2)$ Å and $110.89(2)^\circ$, respectively. In other words, it is still possible to obtain a correct structure using the inaccurate SE A constant.

5. DISCUSSION

An accurate equilibrium structure for propene invites a comparison of the effects of substitution in ethylene on CH bond parameters. Accurate equilibrium structures are available for ethylene,⁴⁷ butadiene,⁴⁷ *trans*-hexatriene,⁴⁸ and *cis*-hexatriene.⁴⁹ Table 8 supplies a comparison of CH bond lengths and C=CH bond angles in the various molecules. The CH_t bond is least affected by the single substitution. Its bond length changes less than 0.0015 Å, mostly through shrinkage; its bond angle changes less than 0.2° by increasing. The CH_c bond increases by up to 0.0025 Å; the C=CH_c bond angle decreases by up to 0.37° . Movement of the hydrogen atom of the CH_c bond toward the substituent is surprising. The largest effect of substitution in ethylene occurs in the parameters of the CH_g bond. The bond length increases up 0.0045 Å. The C=CH_g angle decreases as much as 2.54° in propene. The increase in the CH_g bond length and the decrease in the C=CH_g bond

Table 8. Variation in CH Bond Lengths and C=CH Angles in Substituted Ethylene (in Å)

	CH _g	CH _l	CH _c	C=CH _g	C=CH _l	C=CH _c
CH ₂ =CH ₂ ^a	1.0805	1.0805	1.0805	121.34	121.34	121.34
CH ₂ =CHCH ₃ ^b	1.085	1.081	1.082	118.80	121.41	121.15
CH ₂ =CHCH=CH ₂ ^a	1.085	1.079	1.082	119.91	121.47	120.97
<i>trans</i> -HTE ^c	1.084	1.079	1.082	119.6	121.4	121.0
<i>cis</i> -HTE ^d	1.0825	1.080	1.083	118.9	121.5	121.0

^aReference 47. ^bThis work. ^cReference 48. ^dReference 49.

angle presumably reflect crowding of the CH_g bond by the CH₃ substituent. High-level electronic structure computations capture all of these changes.^{47–49}

The high-accuracy structure of propene also supports a consideration of the bond parameters in the CH₃ group. The notable preference in propene for a CH bond of the CH₃ group being *cis* to the C=C bond can be rationalized by a favorable overlap between the π component of the C=C bond and some π character in the two out-of-plane CH bonds.⁵⁰ A consequence would be somewhat longer CH_a bonds because of greater p character in the contributing carbon orbital than that in the CH_s orbital. Indeed, $r(\text{CH}_s)$ is less than $r(\text{CH}_a)$ in propene (Table 7). Repulsion between the electron density in the CH_s bond and the C=C bond would cause the CCH_s bond angle to increase relative to the CCH_a angle. In Table 7, $\alpha(\text{CCH}_s)$ is greater than $\alpha(\text{CCH}_a)$.

6. CONCLUSIONS

Ground-state rotational and centrifugal distortion constants were determined for the two conformers of propene-3-*d*₁ (CH₂=CHCH₂D). The nuclear quadrupole hyperfine structure due to deuterium was analyzed for both conformers. The experimental centrifugal distortion constants and quadrupole constants were found to be in good agreement with the values calculated *ab initio*. For the A conformer with the CD bond out of plane, a small tunneling splitting was observed and analyzed using a phenomenological IAM treatment. This analysis led to the conclusion that a standard centrifugal distorted Hamiltonian (Watsonian) may be used to derive accurate rotational constants for the A conformer as well as the S conformer (CD bond in plane). The energy difference of the two conformers was also computed *ab initio*, and the conformers were found to be almost isoenergetic. The potential barrier to internal rotation V_3 was also computed *ab initio* and was found to be the dominant term in the potential energy expansion. The anharmonic force field up to semidiagonal quartic terms was calculated at different levels of theory, and its accuracy was established. Finally, an accurate SE equilibrium structure was determined and compared to the theoretical BO structure. The accuracy of the SE structure was furthermore confirmed by using the method of POs. An anomalous isotopic shift was observed for the equilibrium A rotational constant of the A species, but this discrepancy does not significantly affect the accuracy of the structure. The most likely explanation for this anomaly is a small inaccuracy in the calculation of the rovibrational correction.

■ ASSOCIATED CONTENT

Supporting Information

The Supporting Information is available free of charge on the ACS Publications website at DOI: 10.1021/acs.jpca.7b01470.

Appendices I and II, describing special methods for calculations, Figure S1a,S1b showing the gas-phase IR spectrum of propene-3-*d*₁, Table S1 with the structures computed for the maximum in the internal rotation barrier and the minimum energy form in comparison with the SE structure, Table S2 comparing the experimental centrifugal distortion constants with those computed at various levels of theory, Table S3 comparing vibrational wavenumbers and intensities observed in the IR spectrum for propene with predictions at several levels of theory, Table S4 comparing observed and predicted vibration–rotation interaction constants for the torsion mode (ν_{21}), Table S5 comparing computed rovibrational contributions to A_0 , B_0 , and C_0 for two levels of theory, Table S6 showing all of the equilibrium rotational constants and their deviations in two levels of fitting the SE structure, and Table S7 comparing Cartesian coordinates at different levels (PDF)

■ AUTHOR INFORMATION

Corresponding Authors

*E-mail: Jean.Demaison@gmail.com (J.D.).

*E-mail: Norm.Craig@oberlin.edu (N.C.C.).

ORCID

Norman C. Craig: 0000-0003-2864-1910

Notes

The authors declare no competing financial interest.

■ ACKNOWLEDGMENTS

We are grateful to Peter Groner for redoing the fit of the MW lines for the normal species of propene with his ERHAM program. The Department of Chemistry and Biochemistry at Oberlin College supported the synthetic work, and the Department of Chemistry at Kent State University supported the MW investigation. A.G.C. thanks the NKFIH for financial support (Grant No. K119658). The project received additional support from the COST Action CM1405, MOLIM: Molecules in Motion.

■ REFERENCES

- (1) Marcelino, N.; Cernicharo, J.; Agúndez, M.; Roueff, E.; Gerin, M.; Martín-Pintado, J.; Mauersberger, R.; Thum, C. Discovery of Interstellar Propylene (CH₂CHCH₃): Missing Links in Interstellar Gas-Phase Chemistry. *Astrophys. J.* **2007**, *665*, L127–L130.
- (2) Nixon, C. A.; Jennings, D. E.; Bézard, B.; Vinatier, S.; Teanby, N. A.; Sung, K.; Ansty, T. M.; Irwin, P. G. J.; Gorius, N.; Cottini, V.; Coustenis, A.; Flasar, F. M. Detection of Propene in Titan's Stratosphere. *Astrophys. J., Lett.* **2013**, *776*, L14–L19.
- (3) Lide, D. R.; Mann, D. E. Microwave Spectra of Molecules Exhibiting Internal Rotation. I. Propylene. *J. Chem. Phys.* **1957**, *27*, 868–873.
- (4) Craig, N. C.; Groner, P.; Conrad, A. R.; Gurusinge, R.; Tubergen, M. J. Microwave Spectra for the Three ¹³C₁ Isotopologues

of Propene and New Rotational Constants for Propene and its $^{13}\text{C}_1$ Isotopologues. *J. Mol. Spectrosc.* **2016**, *328*, 1–6.

(5) Demaison, J.; Rudolph, H. D. Ab Initio Anharmonic Force Field and Equilibrium Structure of Propene. *J. Mol. Spectrosc.* **2008**, *248*, 66–76.

(6) Demaison, J. The Method of Least Squares. In *Equilibrium Molecular Structures*; Demaison, J., Boggs, J. E., Császár, A. G., Eds.; CRC Press: Boca Raton, FL, 2011; pp 29–52.

(7) Vogt, N.; Demaison, J.; Cocinero, E. J.; Écija, P.; Lesarri, A.; Rudolph, H. D.; Vogt, J. The Equilibrium Molecular Structures of 2-Deoxyribose and Fructose by the Semiexperimental Mixed Estimation Method and Coupled-Cluster Computations. *Phys. Chem. Chem. Phys.* **2016**, *18*, 15555–15563.

(8) Vogt, N.; Demaison, J.; Vogt, J.; Rudolph, H. D. Why it is Sometimes Difficult to Determine the Accurate Position of a Hydrogen Atom by the Semiexperimental Method: Structure of Molecules Containing the OH or the CH_3 Group. *J. Comput. Chem.* **2014**, *35*, 2333–2342.

(9) Piccardo, M.; Penocchio, E.; Puzzarini, C.; Biczysko, M.; Barone, V. Semi-Experimental Structure Determinations by Employing B3LYP/SNSD Anharmonic Force Fields: Validation and Application to Semirigid Organic Molecules. *J. Phys. Chem. A* **2015**, *119*, 2058–2082.

(10) Suenram, R. D.; Grabow, J.-U.; Zuban, A.; Leonov, I. A Portable, Pulsed-Molecular-Beam, Fourier-Transform Microwave Spectrometer Designed for Chemical Analysis. *Rev. Sci. Instrum.* **1999**, *70*, 2127–2135.

(11) Conrad, A. R.; Teumelsan, N. H.; Wang, P. E.; Tubergen, M. J. A Spectroscopic and Computational Investigation of the Conformational Structural Changes Induced by Hydrogen Bonding Networks in the Glycidol-Water Complex. *J. Phys. Chem. A* **2010**, *114*, 336–342.

(12) Kohn, W.; Sham, L. Self-Consistent Equations Including Exchange and Correlation Effects. *J. Phys. Rev. A* **1965**, *140*, 1133–1138.

(13) Becke, A. D. Density-Functional Thermochemistry. III. The Role of Exact Exchange. *J. Chem. Phys.* **1993**, *98*, 5648–5652.

(14) Lee, C. T.; Yang, W. T.; Parr, R. G. Development of the Colle-Salvetti Correlation-Energy Formula into a Functional of the Electron Density. *Phys. Rev. B: Condens. Matter Mater. Phys.* **1988**, *37*, 785–789.

(15) Wong, M. W. Vibrational Frequency Prediction Using Density Functional Theory. *Chem. Phys. Lett.* **1996**, *256*, 391–399.

(16) Bauschlicher, C. W.; Ricca, A.; Partridge, H.; Langhoff, S. R. In *Recent Advances in Density Functional Methods*; Chong, D. P., Eds.; World Scientific: Singapore, 1997; pp 165–227.

(17) Dunning, T. H., Jr. Gaussian Basis Sets for Use in Correlated Molecular Calculations. I. The Atoms Boron through Neon and Hydrogen. *J. Chem. Phys.* **1989**, *90*, 1007–1023.

(18) Møller, C.; Plesset, M. S. Note on an Approximation Treatment for Many-Electron Systems. *Phys. Rev.* **1934**, *46*, 618–622.

(19) Purvis, G. D., III; Bartlett, R. J. A Full Coupled-Cluster Singles and Doubles Model: The Inclusion of Disconnected Triples. *J. Chem. Phys.* **1982**, *76*, 1910–1918.

(20) Raghavachari, K.; Trucks, G. W.; Pople, J. A.; Head-Gordon, M. A Fifth-Order Perturbation Comparison of Electron Correlation Theories. *Chem. Phys. Lett.* **1989**, *157*, 479–483.

(21) Peterson, K. A.; Dunning, T. H., Jr. Accurate Correlation Consistent Basis Sets for Molecular Core–Valence Correlation Effects: The Second Row Atoms Al–Ar, and the First Row Atoms B–Ne Revisited. *J. Chem. Phys.* **2002**, *117*, 10548–10560.

(22) Frisch, M. J.; Trucks, G. W.; Schlegel, H. B.; Scuseria, G. E.; Robb, M. A.; Cheeseman, J. R.; Scalmani, G.; Barone, V.; Mennucci, B.; Petersson, G. A.; et al. *Gaussian 09*, revision E.01; Gaussian, Inc.: Wallingford, CT, 2013.

(23) Stanton, J. F.; Gauss, J.; Harding, M. E.; Szalay, P. G. with contributions from Auer, A. A.; Bartlett, R. J.; Benedikt, U.; Berger, C.; Bernholdt, D. E.; Bomble, Y. J.; et al. *CFOUR, a Quantum Chemical Program Package for Performing High-Level Quantum Chemical Calculations on Atoms and Molecules*; For the current version, see <http://www.cfour.de>.

(24) Gauss, J.; Stanton, J. F. Analytic CCSD(T) Second Derivatives. *Chem. Phys. Lett.* **1997**, *276*, 70–77.

(25) Stanton, J. F.; Gauss, J. Analytic Second Derivatives in High-Order Many-Body Perturbation and Coupled-Cluster Theories: Computational Considerations and Applications. *Int. Rev. Phys. Chem.* **2000**, *19*, 61–95.

(26) Watson, J. K. G. Aspects of Quartic and Sextic Centrifugal Effects on Rotational Energy Levels. In *Vibrational Spectra and Structure*; Durig, J. R., Ed.; Elsevier: Amsterdam, The Netherlands, 1977; Vol. 6, pp 1–89.

(27) Margulès, L.; Coudert, L. H.; Møllendal, H.; Guillemin, J.-C.; Huet, T. R.; Janeckova, R. The Microwave Spectrum of the Mono Deuterated Species of Methyl Formate HCOOCH_2D . *J. Mol. Spectrosc.* **2009**, *254*, 55–68.

(28) Hougen, J. T. A Generalized Internal Axis Method for High Barrier Tunneling Problems, as Applied to the Water Dimer. *J. Mol. Spectrosc.* **1985**, *114*, 395–426.

(29) Coudert, L. H.; Hougen, J. T. Tunneling Splittings in the Water Dimer: Further Development of the Theory. *J. Mol. Spectrosc.* **1988**, *130*, 86–119.

(30) Gordy, W.; Cook, R. L. *Microwave Molecular Spectra*; Wiley: New York, 1984; Chapter IX.

(31) Hirota, E. Microwave Spectrum of Propylene. II. Potential Function for the Internal Rotation of the Methyl Group. *J. Chem. Phys.* **1966**, *45*, 1984–1990.

(32) Włodarczyk, G.; Demaison, J.; Heineking, N.; Császár, A. G. The Rotational Spectrum of Propene: Internal Rotation Analysis and ab Initio and Experimental Centrifugal Distortion Constants. *J. Mol. Spectrosc.* **1994**, *167*, 239–247.

(33) Es-sebbar, E.; Alrefae, M.; Farooq, A. Infrared Cross-Sections and Integrated Band Intensities of Propylene: Temperature-Dependent Studies. *J. Quant. Spectrosc. Radiat. Transfer* **2014**, *133*, 559–569.

(34) Demaison, J.; Møllendal, H.; Perrin, A.; Orphal, J.; Kwabia Tchana, F.; Rudolph, H. D.; Willaert, F. Microwave and High Resolution Infrared Spectra of Vinyl Chloride, ab Initio Anharmonic Force Field and Equilibrium Structure. *J. Mol. Spectrosc.* **2005**, *232*, 174–185.

(35) Demaison, J. Ab Initio Anharmonic Force Field and Equilibrium Structure of Vinyl Fluoride and Vinyl Iodide. *J. Mol. Spectrosc.* **2006**, *239*, 201–207.

(36) Zvereva-Loëte, N.; Demaison, J.; Rudolph, H. D. Ab Initio Anharmonic Force Field and Equilibrium Structure of Vinyl Bromide. *J. Mol. Spectrosc.* **2006**, *236*, 248–254.

(37) Wofsy, S. C.; Muentzer, J. S.; Klemperer, W. Hyperfine Structure and Dipole Moment of CH_3D . *J. Chem. Phys.* **1970**, *53*, 4005–4014.

(38) Lide, D. R., Jr.; Christensen, D. Molecular Structure of Propylene. *J. Chem. Phys.* **1961**, *35*, 1374–1378.

(39) Hirota, E.; Hirooka, T.; Morino, Y. Microwave Spectrum of Propylene Direct Determination of the Internal Rotation Splitting for the $\text{CH}_2\text{DCH}=\text{CH}_2$ Species. *J. Mol. Spectrosc.* **1968**, *26*, 351–367.

(40) Hirota, E. Internal Rotation of the Asymmetric Top. Theory and its Application to the Deuterated Propylene $\text{CH}_2\text{DCH}=\text{CH}_2$. *J. Mol. Spectrosc.* **1970**, *34*, 516–527.

(41) Pearson, J. C.; Sastry, K. V. L. N.; Herbst, E.; DeLucia, F. The Millimeter-Wave and Submillimeter-Wave Spectrum of Propylene (CH_3CHCH_2). *J. Mol. Spectrosc.* **1994**, *166*, 120–129.

(42) Vogt, N.; Vogt, J.; Demaison, J. Accuracy of the Rotational Constants. *J. Mol. Struct.* **2011**, *988*, 119–127.

(43) Demaison, J.; Craig, N. C.; Cocinero, E. J.; Grabow, J.-U.; Lesarri, A.; Rudolph, H. D. Semiexperimental Equilibrium Structures for the Equatorial Conformers of N-Methylpiperidone and Tropinone by the Mixed Estimation Method. *J. Phys. Chem. A* **2012**, *116*, 8684–8692.

(44) Kraitchman, J. Determination of Molecular Structure from Microwave Spectroscopic Data. *Am. J. Phys.* **1953**, *21*, 17–24.

(45) Demaison, J.; Craig, N. C.; Conrad, A. R.; Tubergen, M. J.; Rudolph, A. D. Semiexperimental Equilibrium Structure of the Lower Energy Conformer of Glycidol by the Mixed Estimation Method. *J. Phys. Chem. A* **2012**, *116*, 9116–9122.

(46) Demaison, J.; Rudolph, H. D. When Is the Substitution Structure Not Reliable? *J. Mol. Spectrosc.* **2002**, *215*, 78–84.

(47) Craig, N. C.; Groner, P.; McKean, D. C. Equilibrium Structures for Butadiene and Ethylene: Compelling Evidence for Π -Electron Delocalization in Butadiene. *J. Phys. Chem. A* **2006**, *110*, 7461–7469.

(48) Craig, N. C.; Demaison, J.; Groner, P.; Rudolph, H. D.; Vogt, N. Electron Delocalization in Polyenes: A Semiexperimental Structure for (3E)-1,3,5-Hexatriene and Theoretical Structures for (3Z, 5Z)-, (3E,5E)-, and (3E,5Z)-1,3,5,7-Octatetraene. *J. Phys. Chem. A* **2015**, *119*, 195–204.

(49) Craig, N. C.; Chen, Y.; Fuson, H. A.; Tian, H.; van Besien, H.; Conrad, A. R.; Tubergen, M. J.; Rudolph, H. D.; Demaison, J. Microwave Spectra for Deuterium Isotopologues of *cis*-Hexatriene and a Semiexperimental Equilibrium Structure. *J. Phys. Chem. A* **2013**, *117*, 9391–9400.

(50) Anselyn, E. K.; Dougherty, D. A. *Modern Physical Organic Chemistry*; University Science Books: Sausalito, CA, 2006; pp 43–45.